Check for updates

Wiley
Journal of Mathematics
Volume 2025, Article ID 4572689, 10 pages
https://doi.org/10.1155/jom/4572689

WILEY

Research Article

Distance-Normal Congruence of Rotational Surfaces in Euclidean 3-Space

Betül Bulca Sokur

Department of Mathematics, Bursa Uludag University, Bursa, Turkey

Correspondence should be addressed to Betül Bulca Sokur; bbulca@uludag.edu.tr

Received 27 February 2025; Revised 8 July 2025; Accepted 1 August 2025

Academic Editor: Erhan Güler

Copyright © 2025 Betül Bulca Sokur. Journal of Mathematics published by John Wiley & Sons Ltd. This is an open access article under the terms of the Creative Commons Attribution License, which permits use, distribution and reproduction in any medium, provided the original work is properly cited.

In this study, we considered simple linear congruences of some curves/surfaces to generate parametric families of curves/surfaces. The method depends essentially on the position vector of a curve/surface and its signed unit normal. The shape of the normal congruence of the curve/surface can be predictably changed based on the sign of its unit normal. On the other hand, symmetry of surfaces refers to invariance under transformations such as reflections, rotations, or translations, which can also involve normal congruence. Considering the normal congruences of the surface of revolution to be minimal, some results on the meridian curves are obtained. Furthermore, some surface models are constructed over the meridian curves.

Keywords: distance normal; meridian curve; normal congruence; rotational surface

1. Introduction

It is essential to analyze geometric models of curved surfaces for design and manufacturing processes. For example, it is imperative to visualize the technical smoothness of the surfaces and test their convexity [1]. The 3D offset or parallel surfaces have a wide range of applications. As known, often offsetting curves on surfaces is used to generate tool paths for free-form surfaces; however, most of the literature available in this area aims at offsetting 2D and 3D curves and offsetting curves on parametric surfaces.

Tool path generation for 3N machining can be added to these applications. The concept of 3D offsets or parallel surfaces is crucial in both tool path generation for 3-axis (3N) machining and in CAD geometry modifications. However, 3D offsets are also valuable for modifying CAD geometries. 3D offsets allow for the generation of tool paths that follow the contours of complex surfaces, ensuring consistent cutting depths and improved surface finishes. By creating offsets, machines can adapt tool paths to variations in part geometry, enhancing efficiency and reducing wear on tools. However, 3N machining typically refers to 3-axis CNC machining, where tools operate along the three linear axes: *X*, Y, and Z. This is a fundamental technique used in various manufacturing processes. 3N machining is a versatile and widely used method in manufacturing, allowing for the production of a variety of components across different industries. Various tools can be used, including end mills, drills, and reamers, depending on the machining operation. Its straightforward nature makes it an excellent choice for many applications, though considerations around complexity and setup remain important [2–6].

A 3D offset surface (or simply offset surface) is a geometric model generated by shifting each point on a given base surface along its normal vector by a constant or variable distance. Defining the 3D offset model of a surface is possible by moving that surface to a distance of "d" units along the unit normal. Offset surfaces have been considered by the authors in [7, 8]. In general, a 3D model set is obtained to reconstruct a closed 3D model by first aligning all model surfaces and then cutting and expanding these sets [9, 10]. It plays a crucial role in applications such as CNC machining (tool path generation), mold design, reverse engineering, and surface blending. Focal surfaces, known as line

complexes, are highly functional in NC milling. These surfaces have also been used to display the line congruences [1, 11]. In CNC machining, offset surfaces define tool trajectories to maintain constant machining depth. Focal surfaces are an important concept in differential geometry, particularly in the study of curves and surfaces. They can be defined in several contexts, such as in the study of geodesics, wave propagation, or optics.

Generalized focal surfaces are described with the help of a curvature function, which depends on the principal curvatures. If the curvature function is chosen as the inverse of the principal curvatures, focal surfaces are obtained. Generalized focal surfaces are surfaces that represent the set of points where certain geometric conditions related to curvature and focus are met. They can be derived from various geometrical constructs, such as curves and surfaces, and are useful in characterizing complex shapes. Different generalized focal surface models are obtained by different selections of the curvature function. Therefore, generalized focal surfaces form a rich classification in the modeling of surfaces in differential geometry and computing. Generalized focal surfaces represent a significant intersection of geometry, computer science, and engineering. Their ability to model complex shapes and interactions makes them invaluable in various fields, from design to manufacturing and beyond. This method was first discussed in [1, 11]. The focal length, known from linear geometry, is based on selecting a function expressed by principal curvatures.

The rest of this paper is organized as follows. In Section 2, we review the mathematical preliminaries of the normal correspondence of variable curves and surfaces. In Section 3, we obtain some results, showing that the $\rho-$ normal correspondence of regular surfaces is minimal. Furthermore, we build a standard uniform surface on the meridian curves generated by the fitted surface curves. In the context of 3D geometric modeling, a standard uniform surface usually refers to a surface with uniform parameterization and regular structure, typically defined over a rectangular domain. This term is commonly associated with tensor product surfaces, such as uniform B-spline or uniform Bézier surfaces. These uniform surfaces are widely used in computer-aided design (CAD), computer-aided manufacturing (CAM), simulation, and reverse engineering due to their regular structure, smoothness, and mathematical simplicity. All the images in this article were created using the Maple program.

2. Materials and Methods

The main purpose of normal congruence for curves and surfaces is to analyze and understand the geometric properties and behaviors of these shapes. For curves, it helps in visualizing how curves bend and turn by providing insights into their curvature and torsion through the collection of normal lines. For surfaces, normal congruence aids in studying surface properties, such as curvature and orientation, which are essential in fields such as differential geometry, computer graphics, and engineering. By delving into these concepts, one can achieve a deeper understanding of the ultimate geometry involved in various applications, including shape optimization and motion planning. In differential geometry, normal congruences help characterize curves and surfaces through properties such as curvature, which describe how shapes deviate from being flat. This understanding is crucial for formulating geometric theorems and studying the intrinsic properties of surfaces.

In computer graphics, normal congruences are essential for rendering techniques, such as shading and lighting. By calculating normals at surface points, algorithms can simulate how light interacts with surfaces, creating realistic visuals. In addition, normal lines are used in collision detection and mesh processing [4, 12, 13].

In this section, we give the basic properties and basic concepts of normal congruence of planar curves and surfaces in 3-dimensional Euclidean space.

2.1. Normal Congruence of a Plane Curve. Normal congruence of planar curves refers to the collection of all normal lines in a given curve in the plane. The collection of all normal lines at every point of the curve constitutes the normal congruence. This forms a geometric structure that gives insight into the behavior of the curve at various points. Each point on the curve contributes a normal line, and the set of all these lines describes how the curve bends and changes direction. Normal congruence captures the idea of all normal lines to a planar curve, providing a rich geometric framework for analysis and application. Normal congruences are useful in various fields such as computer graphics, robotics, mechanics, optics, and differential geometry, where understanding the orientation and shape of curves is essential.

Let x be a regular planar curve. Given a point $x(t)$, and using the fact that $\rho(x)$ is the signed distance to the closest point on the interface, we can write

$$\tilde{x}(t) = x(t) - \rho(x)N(t), \tag{1}$$

to calculate the closest point to the interface, where N is the local unit normal at $x(t)$. Again, this is true only in the general case, since equidistant points $x(t)$ have more than one closest point $\tilde{x}(t)$. Also, on our Cartesian grid, equation (1) will be only an approximation of the closest point on the interface $\tilde{x}(t)$. The geometric location of the points defined by equation (1) is expressed as the normal congruence of the curve x.

Depending on the type of the signed distance function $\rho(x)$, the following special cases occur:

i. If $\rho(x)$ is a constant function, then the normal congruence $\tilde{x}(t)$ is called the parallel (offset) of the base curve $x(t)$. Parallel curves in the plane and their spline approximations have been extensively studied for their use in creating tool paths for CNC machines [14, 15]. Parallel processes often make use of the stylistic features of the artistic intent that appear in different contexts, but especially in the design of revolutionary surfaces such as vases and plates.

14690, 2025, 1, Downloaded from https://onlinelibrary.wiley.com/doi/10.1155/jom/4572689 by Betul Bulca - Bursa Uludag University Kutuphane ve Dokumantasyon , Wiley Online Library on [25/08/2025]. See the Terms and Conditions (https://onlinelibrary.wiley.com/terms-and-conditions) on Wiley Online Library for rules of use; OA articles are governed by the applicable Creative Commons License

ii. If $(x) = 1/\kappa$, then the normal congruence $\tilde{x}(t)$ is called the evolute (or focal curve) of the base curve $x(t)$. Here, κ is the (signed) curvature of $x(t)$ defined by

$$\kappa = \frac{\langle \gamma''(t), J(\gamma'(t)) \rangle}{\|\gamma'(t)\|^3}, \tag{2}$$

where $J(\gamma'(t))$ is the rotation of $\gamma'(t)$ with an angle of $\pi/2$ in the counterclockwise direction, and the norm (or length) is defined as

$$\|\gamma'(t)\| = \sqrt{(\gamma_1')^2(t) + (\gamma_2')^2(t)}. \tag{3}$$

Classically, an evolute is known to be an envelope of a family of normal lines along a curve γ [16, 17]. In this case, the envelope of the tangent along γ is the original curve, and the sum of the tangents at each inflection point is γ. In 2014, Giblin and Warder introduced the concept of evolution as a family of single-parameter paired γ curves that bridge the gap between the evolution curve and the original curve [18]. Each member of the evolution diagram is defined as an envelope of a family of lines, so that each line has a fixed angle to the tangent at the same point on the original curve. In the present study, we add a new signed distance function to the above list by

$$\rho(x) = \|x(t)\|, \tag{4}$$

which is the distance function on the base curve x. Consequently, the ρ-normal congruence of the base curve x will have the parametrization

$$\tilde{x}(t) = x(t) - \|x(t)\| N(t). \tag{5}$$

2.2. Normal Congruences of Surfaces. Normal congruence of surfaces refers to the collection of all normal lines at points on a surface. The normal lines provide insight into how the surface bends and curves. They can be visualized as lines extending outwards from the surface, indicating the orientation of the surface at each point. Overall, normal congruences provide a framework for both theoretical exploration and practical applications, making them a cornerstone concept in differential geometry and related fields.

The general focus is on a surface research method. The concept of common foci is crucial to hedgehog diagrams. Instead of drawing a surface normal proportional to the value of the function, only a point is drawn on the surface normal that is proportional to the function. The locations of all these points form the common focal length. This method was introduced by Hagen and Hahmann in [1] and is based on the concept of focal planes known from linear geometry. Focal surfaces are the locations of a given concordance line, all focal points of a normal concordance. Given a set of unit vectors $E(u, v)$, one can define a ρ-line congruence as follows:

$$\tilde{x}(u, v) = x(u, v) - \rho(u, v) E(u, v), \tag{6}$$

where $\rho(u, v)$ is called the signed distance (offset) function between $x(u, v)$ and $E(u, v)$. If $E(u, v) = N(u, v)$, then $\tilde{x}$ is called a ρ-normal congruence of x. Here, $x(u, v)$ is called the base surface. Depending on the type of $\rho(u, v)$, the following special cases occur:

i. If $\rho(u, v)$ is a constant function, then the normal congruence $\tilde{x}(u, v)$ is called the parallel (offset) surface of the base surface $x(u, v)$.

ii. If $\rho(u, v) = 1/\kappa_i$, then the normal congruence $\tilde{x}(u, v)$ is called the evolute (or focal surfaces) of the base surface $x(u, v)$. Here, $\kappa_i, i = 1, 2$ are the principal curvatures of $x(u, v)$.

iii. If $\rho(u, v) = \kappa_1 \kappa_2$, then $\tilde{x}(u, v)$ is called the Gaussian-normal congruence of $x(u, v)$.

iv. If $\rho(u, v) = (1/2)(\kappa_1 + \kappa_2)$, then $\tilde{x}(u, v)$ is called the mean-normal congruence of $x(u, v)$.

v. If $\rho(u, v) = (\kappa_1^2 + \kappa_2^2)$, then $\tilde{x}(u, v)$ is called the energy functional–normal congruence of $x(u, v)$.

vi. If $\rho(u, v) = |\kappa_1| + |\kappa_2|$, then $\tilde{x}(u, v)$ is called the absolute-normal congruence of $x(u, v)$.

vii. If $(u, v) = \kappa_i$, then $\tilde{x}(u, v)$ is called the principle-normal congruence of $x(u, v)$.

The normal congruence defined between (iii) and (vii) is also called the generalized focal surfaces of the base surface $x(u, v)$ [19]. The different values of $\rho(u, v)$ listed above can be used to interrogate and visualize surfaces with respect to the following criteria [19]:

- Convexity test
- Detection of flat points
- Detection of surface integration
- Visualization of curvature behavior
- Visualization of technical smoothness
- Visualization of C^2 and C^3 discontinuities
- Test of technical aspects

In the present study, we add a new signed distance function to the above list by

$$\rho(u, v) = \|x(u, v)\|. \tag{7}$$

Consequently, the ρ-normal congruence of the base surface x will have the parametrization of the form

$$\tilde{x}(u, v) = x(u, v) - \|x(u, v)\| N(u, v). \tag{8}$$

3. Results

Rotational hypersurfaces are one of the important topics of modern differential geometry. These hypersurfaces are widely used in $\mathbb{R}^3$, especially in computer-aided geometric design (CAGD) and surface modeling. Rotational surfaces, also known as surfaces of revolution, are surfaces generated by rotating a curve (the generatrix) around a straight line

14690, 2025, 1, Downloaded from https://onlinelibrary.wiley.com/doi/10.1155/jom/4572689 by Betul Bulca - Bursa Uludag University Kutuphane ve Dokumantasyon , Wiley Online Library on [25/08/2025]. See the Terms and Conditions (https://onlinelibrary.wiley.com/terms-and-conditions) on Wiley Online Library for rules of use; OA articles are governed by the applicable Creative Commons License

(the axis of rotation). Surfaces of revolution constitute the most easily recognized surface class. Their importance spans various fields, including mathematics, physics, engineering, and computer graphics. Since ancient times, surfaces of revolution are not only well known but also common in geometric modeling, because they can be found everywhere in nature. For instance, in human artifacts, in technical practice, and also in mathematics. Moreover, many objects from everyday life such as cans, table glasses, and furniture legs. They are examples of surfaces of revolution. Also, the process of lathing wood produces surfaces of revolution by its very nature [20, 21].

In this subsection, original results regarding the cases of rotational hypersurfaces with ρ-normal congruence are obtained, and some examples supporting these results are given. Because the normal congruence of rotational surfaces provides critical information about their geometry, it influences various applications in engineering, graphics, and physical sciences.

Let $\gamma(u) = (f(u), g(u))$ be a smooth curve in the plane $z = 0$ in $\mathbb{R}^3$ parametrized by the arc length u. We will assume that the domain, where u is defined, is an interval I, and that $g(u) > 0$ on I. We will denote a rotational surface M in $\mathbb{R}^3$, whose generating curve is $\gamma(u)$ and whose rotational axis is the x-axis, by

$$x(u, v) = (f(u), g(u)\cos v, g(u)\sin v), \tag{9}$$

where $\gamma(u)$ is the meridian curve of M [22]. The orthonormal frame field of M is spanned by the vector fields

$$\begin{aligned} e_1 &= \frac{1}{\varphi(u)}\frac{\partial x}{\partial u}, \\ e_2 &= \frac{1}{g(u)}\frac{\partial x}{\partial v}, \\ N &= \frac{1}{\varphi(u)}\left(g'(u), -f'(u)\cos v, -f'(u)\sin v\right), \end{aligned} \tag{10}$$

where φ is the differentiable function defined by [23]

$$\varphi(u) = \sqrt{f'(u)^2 + g'(u)^2}. \tag{11}$$

The second partial derivatives of $x(u, v)$ are expressed as follows:

$$\begin{aligned} x_{uu} &= \left(f''(u), g''(u)\cos v, g''(u)\sin v\right), \\ x_{uv} &= \left(0, -g'(u)\sin v, g'(u)\cos v\right), \\ x_{vv} &= (0, -g(u)\cos v, -g(u)\sin v). \end{aligned} \tag{12}$$

So, the coefficients of the second fundamental form of the surface are

$$\begin{aligned} L_{11} &= \frac{k}{\varphi}, \\ L_{12} &= 0, \\ L_{22} &= \frac{f'g}{\varphi}, \end{aligned} \tag{13}$$

where $k = f''g' - f'g''$ is the differentiable function. Furthermore, the Gaussian and mean curvatures of the surface become

$$K = \frac{kf'}{g\varphi^4}, \tag{14}$$

and

$$H = \frac{kg + f'\varphi^2}{2g\varphi^3}. \tag{15}$$

The ρ-normal congruence of M is given by

$$\begin{aligned} \widetilde{M}\colon \tilde{x}(u, v) &= x(u, v) - \rho N(u, v) \\ &= \left(f - \frac{\rho g'}{\varphi}, \left(g + \frac{\rho f'}{\varphi}\right)\cos v, \left(g + \frac{\rho f'}{\varphi}\right)\sin v\right), \end{aligned} \tag{16}$$

where

$$\rho = \|x(u, v)\| = \sqrt{f(u)^2 + g(u)^2}, \tag{17}$$

is the distance function of M. Furthermore, using

$$\begin{aligned} \tilde{f}(u) &= f(u) - \rho(u)\frac{g'(u)}{\varphi(u)}, \\ \tilde{g}(u) &= g(u) + \rho(u)\frac{f'(u)}{\varphi(u)}, \end{aligned} \tag{18}$$

the parametrization (16) of the ρ-normal congruence $\widetilde{M}$ turns into

$$\widetilde{M}\colon \tilde{x}(u, v) = (\tilde{f}(u), \tilde{g}(u)\cos v, \tilde{g}(u)\sin v). \tag{19}$$

The orthonormal frame field of $\widetilde{M}$ is spanned by the vector fields

$$\begin{aligned} \tilde{e}_1 &= \frac{1}{\tilde{\varphi}(u)}\frac{\partial \tilde{x}}{\partial u}, \\ \tilde{e}_2 &= \frac{1}{\tilde{g}(u)}\frac{\partial \tilde{x}}{\partial v}, \\ \tilde{N} &= \frac{1}{\tilde{\varphi}(u)}\left(\tilde{g}'(u), -\tilde{f}'(u)\cos v, -\tilde{f}'(u)\sin v\right), \end{aligned} \tag{20}$$

where $\tilde{\varphi}$ is the differentiable function defined by

$$\tilde{\varphi} = \sqrt{\tilde{f}'(u)^2 + \tilde{g}'(u)^2}. \tag{21}$$

However, with the help of the second partial derivatives of $\tilde{x}$, the second fundamental form coefficients of $\widetilde{M}$ are calculated as

1469, 2025, 1, Downloaded from https://onlinelibrary.wiley.com/doi/10.1155/jom/4572689 by Betul Bulca - Bursa Uludag University Kutuphane ve Dokumantasyon , Wiley Online Library on [25/08/2025]. See the Terms and Conditions (https://onlinelibrary.wiley.com/terms-and-conditions) on Wiley Online Library for rules of use; OA articles are governed by the applicable Creative Commons License

$$\widetilde{L}_{11} = \left\langle \widetilde{x}_{uu}, \widetilde{N} \right\rangle = \frac{\widetilde{k}}{\widetilde{\varphi}},$$
$$\widetilde{L}_{12} = \left\langle \widetilde{x}_{uv}, \widetilde{N} \right\rangle = 0, \tag{22}$$
$$\widetilde{L}_{22} = \left\langle \widetilde{x}_{vv}, \widetilde{N} \right\rangle = \frac{\widetilde{f}'\widetilde{g}}{\widetilde{\varphi}},$$

where $\widetilde{k}$ is the differentiable function on $\widetilde{M}$ defined by

$$\widetilde{k} = \widetilde{f}''\widetilde{g}' - \widetilde{f}'\widetilde{g}''. \tag{23}$$

Furthermore, comparing

$$h\left(\widetilde{x}_u, \widetilde{x}_u\right) = \widetilde{L}_{11}\widetilde{N},$$
$$h\left(\widetilde{x}_u, \widetilde{x}_v\right) = \widetilde{L}_{12}\widetilde{N}, \tag{24}$$
$$h\left(\widetilde{x}_v, \widetilde{x}_v\right) = \widetilde{L}_{22}\widetilde{N},$$

with

$$h\left(\widetilde{e}_1, \widetilde{e}_1\right) = h\left(\frac{\widetilde{x}_u}{\left\|\widetilde{x}_u\right\|}, \frac{\widetilde{x}_u}{\left\|\widetilde{x}_u\right\|}\right) = \frac{\widetilde{L}_{11}}{\widetilde{\varphi}^2}\widetilde{N},$$
$$h\left(\widetilde{e}_1, \widetilde{e}_2\right) = h\left(\frac{\widetilde{x}_u}{\left\|\widetilde{x}_u\right\|}, \frac{\widetilde{x}_v}{\left\|\widetilde{x}_v\right\|}\right) = 0, \tag{25}$$
$$h\left(\widetilde{e}_2, \widetilde{e}_2\right) = h\left(\frac{\widetilde{x}_v}{\left\|\widetilde{x}_v\right\|}, \frac{\widetilde{x}_v}{\left\|\widetilde{x}_v\right\|}\right) = \frac{\widetilde{L}_{22}}{\widetilde{g}^2}\widetilde{N},$$

we obtain the coefficients of the second fundamental form of $\widetilde{M}$ by

$$\widetilde{h}_{11} = \frac{\widetilde{k}}{\widetilde{\varphi}^3},$$
$$\widetilde{h}_{12} = \widetilde{h}_{21} = 0, \tag{26}$$
$$\widetilde{h}_{22} = \frac{\widetilde{f}\widetilde{g}}{\widetilde{\varphi}}.$$

Thus, with the help of (26), the shape operator matrix of $\widetilde{M}$ is expressed as

$$A_{\widetilde{N}} = \begin{pmatrix} \widetilde{h}_{11} & \widetilde{h}_{12} \\ \widetilde{h}_{21} & \widetilde{h}_{22} \end{pmatrix} = \begin{pmatrix} \frac{\widetilde{k}}{\widetilde{\varphi}^3} & 0 \\ 0 & \frac{\widetilde{f}'}{\widetilde{g}\widetilde{\varphi}} \end{pmatrix}. \tag{27}$$

Thus, with the help of (27), the following results are obtained.

Lemma 1. *Let $\widetilde{M}$ be the ρ-normal congruence given by parametrization (19). Then, the Gaussian curvature of $\widetilde{M}$ is given by*

$$\widetilde{K} = \det\left(A_{\widetilde{N}}\right) = \frac{\widetilde{f}'\widetilde{k}}{\widetilde{g}\widetilde{\varphi}^4}, \tag{28}$$

where $\widetilde{\varphi}$ and $\widetilde{k}$ are differentiable functions, defined in (21) and (23), respectively.

Lemma 2. *Let $\widetilde{M}$ be the ρ-normal congruence given by parametrization (19). Then, the mean curvature of $\widetilde{M}$ is given by*

$$\widetilde{H} = \frac{1}{2}tr\left(A_{\widetilde{N}}\right) = \frac{\widetilde{k}\widetilde{g} + \widetilde{f}'\widetilde{\varphi}^2}{2\widetilde{g}\widetilde{\varphi}^3}, \tag{29}$$

where $\widetilde{\varphi}$ and $\widetilde{k}$ are differentiable functions, defined in (21) and (23), respectively.

We can examine the case where the meridian curve of the surface M is unit speed and $\widetilde{M}$ is minimal in two stages as follows.

I. Let $\widetilde{f} = c$ be a constant, then $\widetilde{k} = 0$ from (23). Thus, the meridian curve of $\widetilde{M}$ is a straight line, and the surface $\widetilde{M}$ is part of the plane. In this case, from (17),

$$f = \rho g', \tag{30}$$

is obtained. Since the meridian curve of the surface M is of unit speed,

$$\left(f'\right)^2 + \left(g'\right)^2 = 1, \tag{31}$$

holds identically. Thus, we obtain the following system of differential equations:

$$\begin{aligned} \left(f'(u)\right)^2 + \left(g'(u)\right)^2 &= 1, \\ f(u) - \rho(u)g'(u) &= 0. \end{aligned} \tag{32}$$

By the use of the Maple command,

$$\begin{aligned} &> \text{sys} - \text{ode} := \text{diff}\left(f(u), u\right)^2 + \text{diff}\left(g(u), u\right)^2 = 1, \\ &\quad f(u)^2 = \left(f(u)^2 + g(u)^2\right) * \text{diff}\left(g(u), u\right)^2; \\ &> \text{dsolve}\left(\left[\text{sys} - \text{ode}\right]\right), \end{aligned} \tag{33}$$

one can get

$$f(u) = \frac{a}{2}\left(e^{(u+b)/a} - e^{(u-b)/a}\right),$$
$$g(u) = -\frac{f(u)f'(u)}{\sqrt{1 - \left(f'(u)\right)^2}}, \tag{34}$$

or

1469, 2025, 1, Downloaded from https://onlinelibrary.wiley.com/doi/10.1155/jom/4572689 by Betul Bulca - Bursa Uludag University Kutuphane ve Dokumantasyon , Wiley Online Library on [25/08/2025]. See the Terms and Conditions (https://onlinelibrary.wiley.com/terms-and-conditions) on Wiley Online Library for rules of use; OA articles are governed by the applicable Creative Commons License

$$f(u) = \frac{a}{2}\left(e^{-(u+b)/a} - e^{(u+b)/a}\right),$$
$$g(u) = \frac{f(u)f'(u)}{\sqrt{1-\left(f'(u)\right)^2}}, \tag{35}$$

where a and b are integral constants. So, summing up (34) and (35), we obtain the following results.

Theorem 1. *Let $\widetilde{M}$ be a ρ-normal congruence of the rotational surface M. If the meridian curve of $\widetilde{M}$ is a straight line, then the meridian curve of M has the parametrization in (34) or (35).*

II. Let $\widetilde{f} = u$, then from (21), (23), and (29) equations,

$$\widetilde{g}''(u)\widetilde{g}(u) - \left(\widetilde{g}'(u)\right)^2 = 1, \tag{36}$$

is obtained. Thus, a nontrivial solution to this equation is $\widetilde{g}(u) = \cosh(u)$. So, the surface $\widetilde{M}$ is a rotational surface whose meridian curve indicates a catenary, and the surface $\widetilde{M}$ becomes a catenoid. Furthermore, using equation (17), the meridian curve of the surface M must have the parametrization

$$f(u) = \frac{\rho}{\varphi}\sinh(u) + u,$$
$$g(u) = \frac{\rho}{\varphi} + \cosh(u). \tag{37}$$

Thus, we obtain the following result.

Theorem 2. *Let $\widetilde{M}$ be a ρ-normal congruence of the rotational surface M. If the meridian curve of $\widetilde{M}$ represents a catenary, then the meridian curve of M has the parametrization given in (37).*

4. Visualization

It is very important to design objects with uncomplicated methods in CAGD. Therefore, rotational surfaces and their distance-normal congruence are of great importance for this method. In the present section, we give some examples of distance-normal congruences of rotational surfaces in 3-dimensional Euclidean space $\mathbb{R}^3$. Furthermore, making use of the Maple program, we plot the distance-normal congruences of plane curves and their rotational surfaces. Normal congruence surfaces, geometric constructs formed by the normals of a given surface, can play a valuable role in improving design processes and optimizing toolpath planning in CNC machining. Normal congruences represent the direction of surface normals, which can directly inform tool axis orientation in 5-axis machining, which reduces tool wear by maintaining optimal angles between the tool and surface and minimizes undercuts and gouging by adapting tool posture in real time. Also, the envelope or evolute of a normal congruence surface can help evaluate visibility zones, identifying which regions are accessible from given tool orientations. Furthermore, in metrology or reverse engineering, deviations in normal congruences between a reference CAD model and a scanned part can indicate manufacturing defects.

Example 1. An ellipse is defined by the parametrization

$$x(t) = (a\cos t, b\sin t), \tag{38}$$

where a, b are real constants. The distance-normal congruence of this curve is given by

$$\widetilde{x}(t) = \left(\left(a \pm b\frac{\sqrt{a^2\cos^2 t + b^2\sin^2 t}}{\sqrt{b^2\cos^2 t + a^2\sin^2 t}}\right)\cos t, \left(b \pm a\frac{\sqrt{a^2\cos^2 t + b^2\sin^2 t}}{\sqrt{b^2\cos^2 t + a^2\sin^2 t}}\right)\sin t\right), \tag{39}$$

where the sign ± indicates the direction of the unit normal of the ellipse. The graphs of equation (39) are given in Figure 1 for $a = 1, b = 3$. The positive direction was chosen for the left curve, and the negative direction for the right one.

Rotating the ellipse given by (38) about the x-axis, a rotational ellipsoid is obtained. The distance-congruence of this surface and the rotational surface obtained by rotating the curve given by equation (39) about the x-axis is the same (Figure 2).

Example 2. The distance-normal congruence of the curve

$$x(t) = \left(\cos^3 t, \sin^3 t\right), \tag{40}$$

is given by

$$\widetilde{x}(t) = \left(\cos^3 t \pm \sin t\sqrt{\cos^6 t + \sin^6 t}, \sin^3 t \pm \cos t\sqrt{\cos^6 t + \sin^6 t}\right), \tag{41}$$

where the sign ± indicates the direction of the unit normal of the base curve x. The graphs of equation (41) are given in Figure 3. The positive direction was chosen for the left curve, and the negative direction for the right one.

By rotating the plane curve given by equation (40) about the x-axis, a rotational surface is obtained. The distance-congruence of this surface and the rotational surfaces obtained by rotating the curve given by equation (41) about the x-axis is the same (Figure 4).

14690, 2025, 1, Downloaded from https://onlinelibrary.wiley.com/doi/10.1155/jom/4572689 by Betul Bulca - Bursa Uludag University Kutuphane ve Dokumantasyon , Wiley Online Library on [25/08/2025]. See the Terms and Conditions (https://onlinelibrary.wiley.com/terms-and-conditions) on Wiley Online Library for rules of use; OA articles are governed by the applicable Creative Commons License

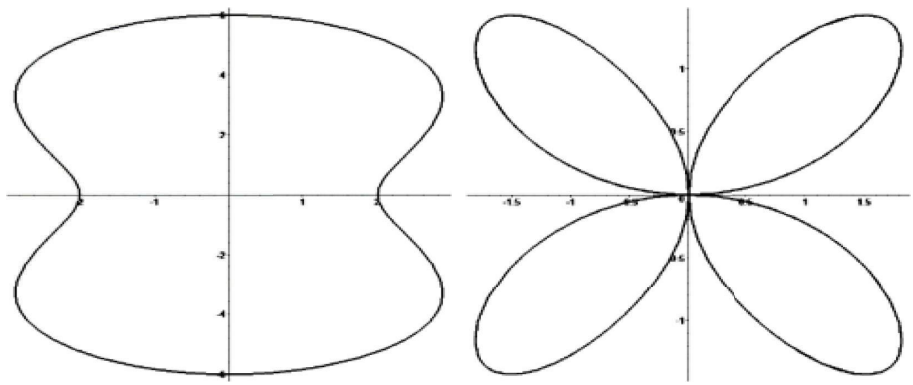

Figure 1: The distance-normal congruence of an ellipse.

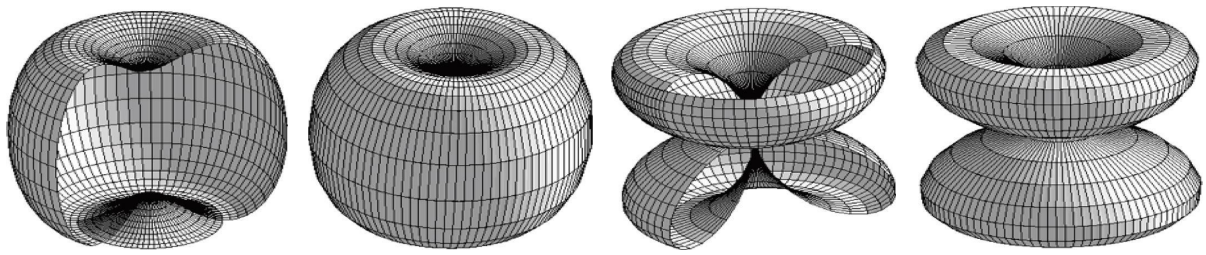

Figure 2: The distance-normal congruence of a rotational ellipsoid.

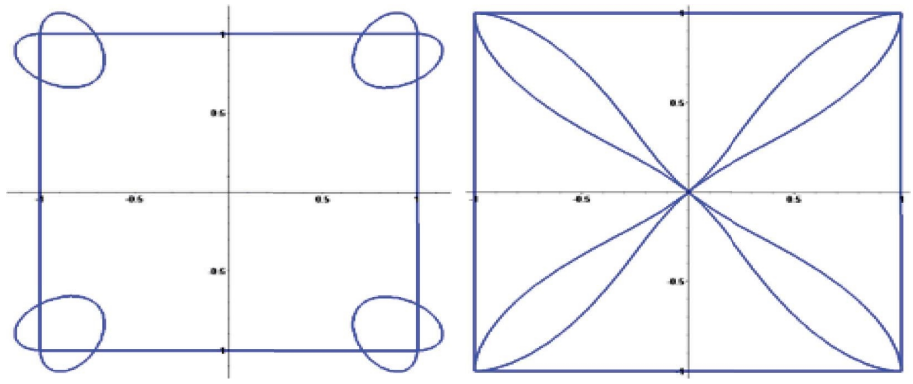

Figure 3: The distance-normal congruence of the curve $x(t) = (\cos^3 t, \sin^3 t)$.

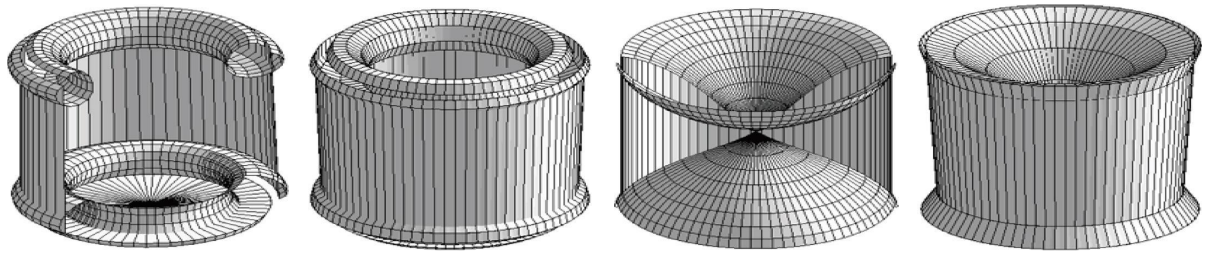

Figure 4: The ρ-normal congruence rotational surfaces of the distance-normal congruence of the curve $x(t) = (\cos^3 t, \sin^3 t)$.

14690, 2025, 1, Downloaded from https://onlinelibrary.wiley.com/doi/10.1155/jom/4572689 by Betul Bulca - Bursa Uludag University Kutuphane ve Dokumantasyon , Wiley Online Library on [25/08/2025]. See the Terms and Conditions (https://onlinelibrary.wiley.com/terms-and-conditions) on Wiley Online Library for rules of use; OA articles are governed by the applicable Creative Commons License

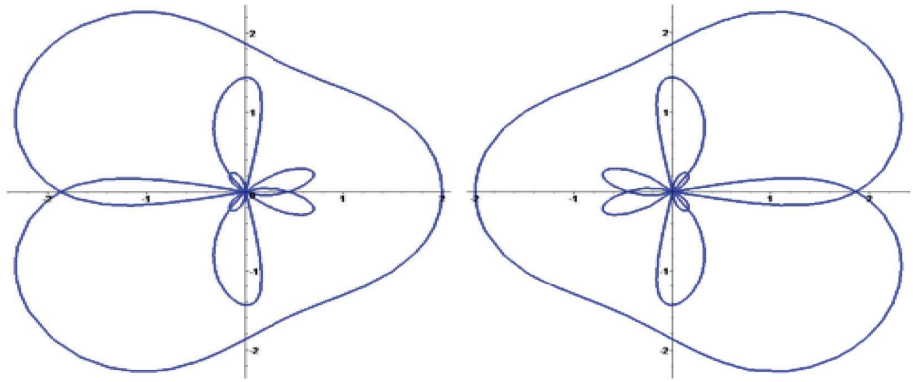

FIGURE 5: The distance-normal congruence of the curve $x(t) = (\cos at, \sin bt)$.

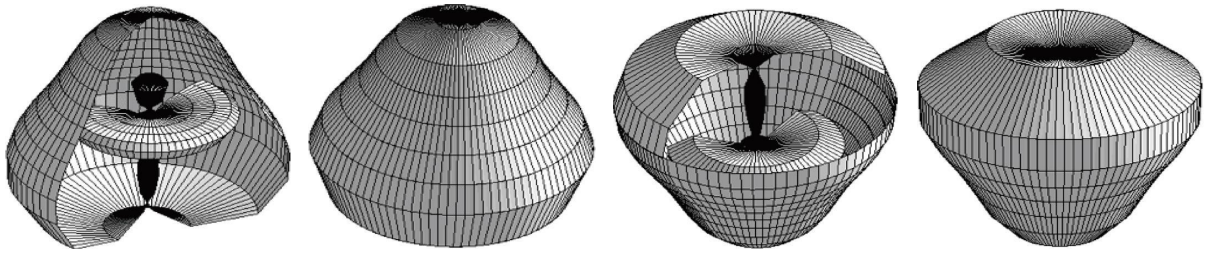

FIGURE 6: The ρ-normal congruence rotational surfaces of the distance-normal congruence of the curve $x(t) = (\cos at, \sin bt)$.

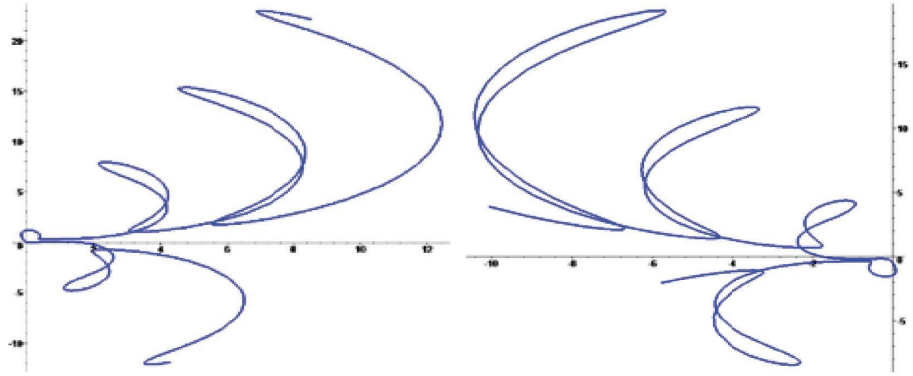

FIGURE 7: The distance-normal congruence of the curve $x(t) = (\cos at, bt + c)$.

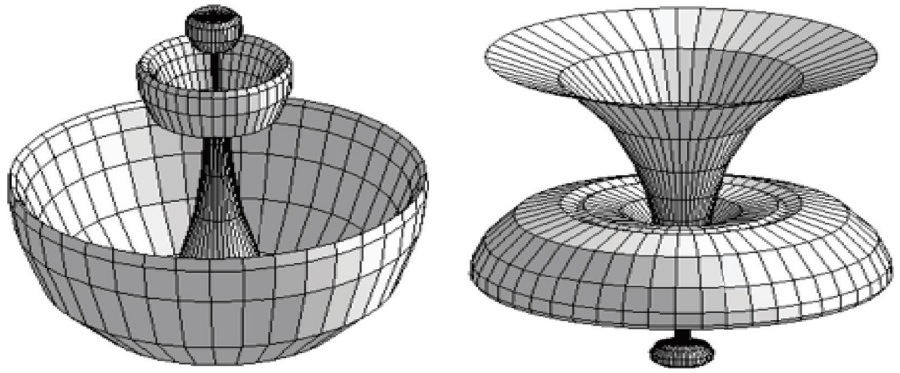

FIGURE 8: The ρ-normal congruence rotational surfaces of the distance-normal congruence of the curve $x(t) = (\cos at, bt + c)$.

1469, 2025, 1, Downloaded from https://onlinelibrary.wiley.com/doi/10.1155/jom/4572689 by Betul Bulca - Bursa Uludag University Kutuphane ve Dokumantasyon , Wiley Online Library on [25/08/2025]. See the Terms and Conditions (https://onlinelibrary.wiley.com/terms-and-conditions) on Wiley Online Library for rules of use; OA articles are governed by the applicable Creative Commons License

Example 3. The distance-normal congruence of the curve

$$x(t) = (\cos at, \sin bt), \tag{42}$$

is given by

$$\tilde{x}(t) = \left(\cos at \pm b \cos bt \frac{\sqrt{\cos^2 at + \sin^2 bt}}{\sqrt{b^2 \cos^2 bt + a^2 \sin^2 at}}, \sin bt \pm a \sin at \frac{\sqrt{\cos^2 at + \sin^2 bt}}{\sqrt{b^2 \cos^2 bt + a^2 \sin^2 at}} \right), \tag{43}$$

where the sign ± indicates the direction of the unit normal of the base curve x. The graphs of equation (43) are given in Figure 5 for $a = 3, b = 2$. The positive direction was chosen for the left curve, and the negative direction for the right one.

By rotating the plane curve given by equation (42) about the x-axis, a rotational surface is obtained. The distance-congruence of this surface and the rotational surfaces obtained by rotating the curve given by equation (43) about the x-axis is the same (Figure 6).

Example 4. The distance-normal congruence of the curve

$$x(t) = (\cos at, bt + c), \tag{44}$$

is given by

$$\tilde{x}(t) = \left(\cos at \pm b \frac{\sqrt{\cos^2 at + (bt + c)^2}}{\sqrt{b^2 + a^2 \sin^2 at}}, bt + c \pm a \sin at \frac{\sqrt{\cos^2 at + (bt + c)^2}}{\sqrt{b^2 + a^2 \sin^2 at}} \right), \tag{45}$$

where the sign ± indicates the direction of the unit normal of the base curve x. The graphs of equation (45) are given in Figure 7 for $a = 3, b = 2$ and $c = 3$. The positive direction was chosen for the left curve, and the negative direction for the right one.

By rotating the plane curve given by equation (44) about the x-axis, a rotational surface is obtained. The distance-congruence of this surface and the rotational surfaces obtained by rotating the curve given by equation (45) about the x-axis is the same (Figure 8).

5. Conclusion

The relationship between normal congruence and symmetry involves how geometric transformations preserve certain properties of curves or surfaces. Both concepts are crucial in understanding geometric invariance but focus on different aspects. Symmetry analysis often identifies the types of transformations that leave an object invariant, while normal congruence involves understanding how those transformations specifically preserve the normal vector field. Normal congruences offer a powerful mathematical framework to describe how waves, light, and particles interact with surfaces or evolve through space.

The concept of a ρ-normal congruence arises in differential geometry and the study of families of curves or surfaces. It involves a congruence (a family of curves or surfaces) that is closely related to the normal lines or normal vectors of a given object, such as a curve or surface. The ρ-normal congruence is often used to describe how a family of curves or surfaces can be defined in terms of distances (often parametrized by a scalar ρ) along the normal direction to a given reference curve or surface.

The ρ-normal congruence can be used to study the focal surfaces and the evolution of geodesics. In particular, this congruence helps describe how the normals to a surface or curve change as you move along them, which is useful in the study of wavefronts, light propagation, and caustics. In computer graphics, the ρ-normal congruence can be used to simulate the effects of displacement or blurring, where the normal direction represents how a surface is perturbed by some external force. Also in optical systems, normal congruences (and their ρ-scaled variants) are useful for understanding how light rays bend, reflect, or refract when interacting with surfaces, especially in the study of wavefronts or focal surfaces [4, 12, 13, 22].

By using the normal congruence method, we produced some parametric curves and surfaces. It has been shown that the normal congruence surfaces of the rotational surface are also rotational surfaces. Normal congruences on rotational surfaces are important for understanding curvature. The normal curvature at a point on the surface can be studied in relation to the principal directions. In addition, the Gaussian and mean curvatures of these surfaces were obtained. However, when normal congruence surfaces are minimal, meridian curves are characterized.

In the visualization part, some surface models were obtained by taking some special curves. These models are considered to be important for CAGD. The collection of all normal lines at each point on the surface can be visualized, providing insights into the surface's geometric properties and how it interacts with other objects or forces. In computer graphics, normal vectors are crucial for rendering surfaces accurately and determining how light interacts with

14690, 2025, 1, Downloaded from https://onlinelibrary.wiley.com/doi/10.1155/jom/4572689 by Betul Bulca - Bursa Uludag University Kutuphane ve Dokumantasyon , Wiley Online Library on [25/08/2025]. See the Terms and Conditions (https://onlinelibrary.wiley.com/terms-and-conditions) on Wiley Online Library for rules of use; OA articles are governed by the applicable Creative Commons License

them. Also, in engineering, designing parts that involve rotational surfaces (e.g., wheels and gears), knowing the normals, helps in analyzing stress and strain.

Data Availability Statement

Data sharing is not applicable as no new data were generated or the article describes entirely theoretical research.

Conflicts of Interest

The author declares no conflicts of interest.

Funding

The author declares that no funds, grants, or other support were received during the preparation of this manuscript.

Acknowledgments

I would like to express my sincere gratitude to all referees who provided valuable feedback on the research and reviewed it.

References

[1] H. Hagen and S. Hahmann, "Generalized Focal Surfaces: a New Method for Surface Interrogation," in *Proceedings of the Visualization* (Boston, United States, 1992).

[2] L. X. Cao and J. Liu, "Computation of Medial Axis and Offset Curves of Curved Boundaries in Planar Domain," *Computer-Aided Design* 40, no. 4 (2008): 465–475, https://doi.org/10.1016/j.cad.2008.01.002.

[3] L. A. Piegl and W. Tiller, "Computing Offsets of NURBS Curves and Surfaces," *Computer-Aided Design* 31, no. 2 (1999): 147–156, https://doi.org/10.1016/s0010-4485(98)00066-9.

[4] B. F. Schutz, *Geometrical Methods of Mathematical Physics* (Cambridge University Press, 1980).

[5] H. Y. Tam, H. W. Law, and H. Y. Xu, "A Geometric Approach to the Offsetting of Profiles on three-dimensional Surfaces," *Computer-Aided Design* 36, no. 10 (2004): 887–902, https://doi.org/10.1016/s0010-4485(03)00151-9.

[6] J. Xu, Y. Sun, and S. Wang, "Tool Path Generation by Offsetting Curves on Polyhedral Surfaces Based on Mesh Flattening," *International Journal of Advanced Manufacturing Technology* 64, no. 9-12 (2013): 1201–1212, https://doi.org/10.1007/s00170-012-4075-6.

[7] T. Maekawa, "An Overview of Offset Curves and Surfaces," *Computer-Aided Design* 31, no. 3 (1999): 165–173, https://doi.org/10.1016/s0010-4485(99)00013-5.

[8] B. Pham, "Offset Curves and Surfaces: a Brief Survey," *Computer-Aided Design* 24, no. 4 (1992): 223–229, https://doi.org/10.1016/0010-4485(92)90059-j.

[9] R. T. Farouki, "Exact Offset Procedures for Simple Solids," *Computer Aided Geometric Design* 2, no. 4 (1985): 257–279, https://doi.org/10.1016/s0167-8396(85)80002-9.

[10] F. Forsty, "Shelling and Offsetting Bodies," in *Proceedings of the 3rd ACM Symposium on Solid Modeling and Applications* (Salt Lake City, Utah, 1995).

[11] H. Hagen, S. Hahmann, and T. Schreiber, "Visualization and Computation of Curvature Behaviour of Freeform Curves and Surfaces," *Computer-Aided Design* 27, no. 7 (1995): 545–552, https://doi.org/10.1016/0010-4485(95)93587-p.

[12] R. S. Millman and G. D. Parker, *Elements of Differential Geometry* (Pearson, 1977).

[13] I. T. Selezov, Y. G. Kryvonos, and I. S. Gandzha, *Wave Propagation and Diffraction: Mathematical Methods and Applications* (Singapore: Springer Nature, 2018).

[14] I. D. Faux and M. J. Pratt, *Computational Geometry for Design and Manufacture* (Ellis Horwood Ltd, 1979).

[15] J. Hoschek, "Spline Approximation of Offset Curves," *Computer Aided Geometric Design* 5, no. 1 (1988): 33–40, https://doi.org/10.1016/0167-8396(88)90018-0.

[16] J. W. Bruce and P. J. Giblin, *Curves and Singularities*, 2nd ed. (Cambridge: Cambridge University Press, 1992).

[17] S. Izumiya, M. A. Romero Fuster, M. A. Soares Ruas, and F. Tari, *Differential Geometry from a Singularity Theory Viewpoint* (Singapore: World Scientific Pub, 2015).

[18] P. J. Giblin and J. P. Warder, "Evolving Evolutoids," *American Mathematical Monthly* 121 (2014): 871–889.

[19] S. Hahmann, "Visualization Techniquies for Surface Analysis," in *Advanced Techniquies, John Viley*, ed. C. Bajaj (1999).

[20] A. Gray, E. Abbena, and S. Salamon, *Modern Differential Geometry of Curves and Surfaces with Mathematica, Third Edition, Studies in Advanced Mathematics* (Boca Raton, FL: Chapman and Hall/CRC, 2006).

[21] J. Vršek and M. Lávička, "Determining Surfaces of Revolution from Their Implicit Equations," *Journal of Computational and Applied Mathematics* 290 (2015): 125–135, https://doi.org/10.1016/j.cam.2015.05.006.

[22] A. Gray, *Modern Differential Geometry of Curves and Surfaces* (CRS Press, Inc, 1993).

[23] B. Bulca, K. Arslan, B. K. Bayram, G. Öztürk, and H. Ugail, "Spherical Product Surfaces in E^3," in *Proceedings of the International Conference on CyberWorlds* (Bradford, UK, 2009).

1469, 2025, 1, Downloaded from https://onlinelibrary.wiley.com/doi/10.1155/jom/4572689 by Betul Bulca - Bursa Uludag University Kutuphane ve Dokumantasyon , Wiley Online Library on [25/08/2025]. See the Terms and Conditions (https://onlinelibrary.wiley.com/terms-and-conditions) on Wiley Online Library for rules of use; OA articles are governed by the applicable Creative Commons License